Clays and Clay Minerals, Vol. 54, No. 6, 678–688, 2006.

ADHERED ZEOLITE PREPARATION ON AND WITHIN A MUSCOVITE MICA BY HYDROTHERMAL GROWTH

CHRISTOPHER D. JOHNSON, ANTHONY J. MALLON AND FRED WORRALL*

Department of Earth Sciences, University of Durham, Science Laboratories, South Road, Durham DH1 3LE, UK

Abstract—Zeolites and other open framework materials provide a powerful tool for remediation and solidification of a range of cationic wastes (*e.g.* NH_4^+, Pb^{2+}) due to the combined properties of large surface area and cation exchange capacity. However, practical barriers exist to the continued expansion of their use, including handling issues related to the fine particle size, and continued ion exchange following waste adsorption. This study examines the synthesis and characterization of zeolites adhered to a muscovite mica wafer, in order to assess if practical benefit can be derived from the preparation of layered composite materials. The paper demonstrates that increased metal adsorption, as demonstrated by surface chemical composition, can be induced in regions by growth of zeolite on and within the lamellar structure of the matrix. X-ray diffraction studies suggest that a site-specific crystallization mechanism controls the zeolite type and extent of growth, thereby reducing control over the zeolites prepared. However, although increased adsorption has been introduced to the mica, the amount of zeolite added is small (<50 mg per gram of muscovite), and thus any adsorption is very limited.

Key Words—Adsorption, Cation, Film, Ion Exchange, Muscovite, Waste, Zeolite.

INTRODUCTION

Zeolites and other porous ion-exchange materials are a potentially powerful tool in environmental management and waste immobilization. Properties linked to the nature and flexibility of the framework have been exploited for a range of proposed applications, including the immobilization of toxic metals within the framework (Johnson *et al.*, 2002), storage of energy (Kyaw *et al.*, 1997), and pervaporative separation (Masuda *et al.*, 2003; Cui *et al.*, 2004a). Current large-scale commercial uses (*e.g.* odor adsorption, fillers in the paper industry, and water treatment), however, rely on more established properties. Principal amongst these are the large adsorption capacity, due to a large surface area, and their ion exchange capacity, linked to the compensation for an overall framework charge. This has led to their use as agents for the separation of gases (Cui *et al.*, 2003, 2004b) and removal of cations from solution (Langella *et al.*, 2000; Sayari *et al.*, 2005).

However, their use as part of a long-term waste disposal solution is limited by the very properties that make them useful. Wastes exchanged or adsorbed onto these materials are easily re-mobilized through continuation of the same process, often brought on by changes in their immediate environment (Xu *et al.*, 1998). Furthermore, this continued exchange can result in leachates which contain far greater concentrations of immobilized cations than were present in the original waste stream. In addition, to this there are physical problems associated with the handling of large volumes of fine powders. Expensive filtration steps are required to separate the zeolite powders from treated liquors, and subsequent handling and disposal routes must take into account the airborne mobility of fine particulate matter and associated health problems resulting from their digestion or inhalation.

Solutions have been proposed for mitigating this release of adsorbed contaminants, including utilizing pore-closure technologies to reduce the availability of adsorbed species, and to reduce ion exchange capacity (Johnson and Worrall, 2004). Although this has been successfully demonstrated, physical abrasion leads to the fresh exposure of zeolite and re-establishment of full ion exchange capacity (Johnson and Worrall, 2004). The use of coarser grains of material (*e.g.* natural zeolite chips or pelletized synthetic zeolite) provides a solution to several of the issues surrounding the handling of fine powders; however, as the kinetics of ion exchange are dependent on the surface area to volume ratio (Johnson *et al.*, 2004), the use of larger zeolite grains compromises the efficiency of the system. Furthermore, pelletization of synthetic zeolites has been shown to offer little improvement over natural granular materials (Mondale *et al.*, 1995).

One potential solution to these problems is the use of zeolites in the form of films adhered to the surface of a support matrix. The zeolite can then behave as a powder, with a large surface area to volume ratio. Although the inclusion of a support matrix reduces the cation exchange capacity of the total material from that observed in a similar weight of pure zeolite, the enhanced structural stability offers some degree of

* E-mail address of corresponding author:
Fred.Worral@durham.ac.uk
DOI: 10.1346/CCMN.2006.0540603

protection against grain fragmentation which occurs as particles in suspension knock against each other. In addition, the anchoring of the zeolite grains to a manipulateable substrate offers a very wide range of potential deployment solutions not available for normal use.

A range of mechanisms exists for the attachment of zeolites to support structures, mainly developed for the separation and catalysis industries (Caro *et al.*, 2000). These mechanisms can be divided into two groups: direct methods including soft solution (Okada *et al.*, 2000) and *in situ* (Okada *et al.*, 2004) methods, and those requiring a secondary hydrothermal treatment, including seeding (Hedlund *et al.*, 1999; Huang *et al.*, 2004; Lassinantti *et al.*, 2000; Cui *et al.*, 2004a), sol-gel routes (Caro *et al.*, 2000), pulsed laser ablation (Deng and Balkus Jr., 2002; Coutinho and Balkus Jr., 2002) and chemical pre-treatments (Caro *et al.*, 2000). Each of these mechanisms has advantages and disadvantages for cost and practicality as well as the level of adhesion of the film (Lassinantti *et al.*, 2000, Okada *et al.*, 2004), and the extent of degradation of the support structure (Okada *et al.*, 2004). For waste management applications it is necessary that the cost is kept to a minimum as an ideal but an expensive solution will always lose out to one which is cheaper but adequate. As a result, the treatment must be simple and the support media efficient (*e.g.* large surface area), cheap and available. This study examines the use of a direct hydrothermal synthesis route to a readily available substrate. The effects of a simple chemical pretreatment applied to the substrate prior to hydrothermal synthesis were also investigated.

The best film adhesion comes from mechanisms where the surface of the support matrix, being chemically similar to the zeolite target, can partially dissolve resulting in growth of a zeolite film integral to the matrix surface, rather than deposited upon it (*e.g. in situ* growth) (Lassinantti *et al.*, 2000; Okada *et al.*, 2004). In this instance, the use of a soft solution/*in situ* approach to a chemically similar substrate has been chosen. Natural sheet silicates (*e.g.* kaolinite) provide an ideal substrate and have been used as zeolite precursors for zeolite synthesis in both film (Okada *et al.*, 2004) and powdered (Murat *et al.*, 1992) form. In these cases treatment with NaOH leads to the formation of zeolite A (Murat *et al.*, 1992). However, kaolinite is a product of hydrothermal weathering of feldspars and other silicates and is a powdery material, unsuitable for use as a support matrix. However, other sheet silicates from the mica group with a similar SiO_2:Al_2O_3 ratio (*e.g.* muscovite) offer the potential for production of large thin plates, due to perfect cleavage, which are mechanically stable, reasonably flexible and abundant.

This study examines whether direct treatment of a muscovite can result in a strongly adhered zeolite film, and what effect the muscovite substrate has on the zeolite formation.

EXPERIMENTAL

All muscovite fragments were collected from a slab containing few visible mineral inclusions. Samples were cleaved along natural cleavage planes until wafers <0.52 mm thick had been produced. These were then cut into squares of ~1 cm^2 in area. The samples were then prepared for the study by examining the pieces under a reflected light microscope and removing by hand any remaining loose fragments, in order to produce upper and lower surfaces as free from major defects as possible. Each wafer was then weighed on a microgram balance prior to any further treatment.

This study examined the effects of two chemical treatments on the muscovite wafers prepared, both individually and in combination. These treatments were:

Treatment with tetraethyl orthosilicate

A selection of prepared muscovite wafers was treated by soaking the pieces for 12 h in tetraethyl orthosilicate (TEOS) before being dried at 85ºC. This was done to examine any improvements in zeolite growth or adhesion resulting from changing the surface chemical characteristics, by deposition of an extremely thin layer of silica on the muscovite surface.

Hydrothermal growth

Muscovite wafers were placed on the surface of 1 cm^2 sections of glass slide and held in place by a crocodile clip which held both glass and muscovite by the edges. A synthesis gel was then prepared, based on a secondary hydrothermal treatment published by Coutinho and Blakus Jr. (2002). This treatment was selected as it had been shown to lead to appropriate zeolite films (zeolite X) being grown. Zeolite X was not a specific target for this study. Solution A was prepared by mixing 2.4 g of NaOH (GPR grade pellets) with 3 g of silica gel (Sigma-Aldrich Davsil Grade 710) in a 60 mL bottle (wide mouth HDPE). To this, 6 mL of deionized water were added, and the sample was shaken gently. Solution B was prepared in a 50 mL glass conical flask by adding 0.57 g of NaOH to 3.15 g of $Na_2O{\cdot}Al_2O_3$ (Alfa Aesar, Technical Grade) followed by 9 mL of deionized water. Great care must be taken following addition of water as the build up of excess heat can lead to hot viscous fluids being ejected from the containers. After 20 min, both mixtures had become viscous solutions which had cooled to room temperature. Solution B was then added to solution A, along with a further 20 mL of deionized water which had been used to rinse the conical flask. On mixing, a white gel formed immediately; the bottles were then sealed and shaken vigorously. The clips were suspended on PTFE ribbon in the hydrothermal treatment gel ~1 cm from the bottom of the bottle with the muscovite downmost. The bottles were resealed and placed in an oven at 80ºC for 36 h during which the gel separated into a fine powder and

https://doi.org/10.1346/CCMN.2006.0540603 Published online by Cambridge University Press

supernatant mother liquor solution. After the transformation of the synthesis gel, the muscovite wafers remained suspended within the powder section rather than in the supernatant fluid.

Following this hydrothermal treatment the bottles were taken from the oven and the muscovite samples removed from the bottles and washed with a jet of deionized water to remove loose material. The muscovite pieces were then removed from the glass plates and dried at 80ºC. The residual powder from the hydrothermal synthesis was separated by vacuum filtration, after the supernatant fluid had cooled to room temperature, and then washed with deionized water before being dried at 80ºC.

The combinations of the described treatments resulted in four sample types which are considered in this study: (1) control (Musc) – the control samples were muscovite wafers prepared as previously described with no chemical treatment; (2) TEOS-only (TEOS) – these samples consisted of wafers which, following preparation, underwent the TEOS treatment only, and were examined in order to investigate the effect of the TEOS treatment on the muscovite wafer; (3) TEOS with hydrothermal treatment (TEOS-Hyd) – these samples underwent the TEOS treatment, followed by hydrothermal treatment. These wafers were used to examine the effects of coating the muscovite surface with silica on the hydrothermal processes, and to determine whether this provides a surface activation for subsequent zeolite formation, or if it reduces the variety of sites of crystal nucleation. (4) Hydrothermal treatment (Hyd) – these wafers were treated with the hydrothermal treatment program only, and offer a comparison with the TEOS-Hyd samples in terms of nucleation site variety and chemical composition of the immediate surface.

All treated wafers were re-weighed after treatment to ascertain the mass of any additional material which had been deposited. Following this, all muscovite wafers, regardless of treatment, and residual powders were analyzed by powder X-ray diffraction (XRD) using a Bruker D8 diffractometer with Sol-X energy dispersive detector (CuKα radiation, step scan 4–60º2θ, step size 0.02º2θ, count time 4 s per step). All samples were rotated continuously throughout sample measurement. Powder samples were placed in bulk holders and illuminated with a variable slit (constant 202 mm × 202 mm illumination). Wafers were mounted on a flat surface using petroleum jelly, and were illuminated with a variable slit (constant 42 mm × 42 mm illumination). A ground randomized sample of muscovite was prepared and mounted on a holder using petroleum jelly. This sample was illuminated with a variable slit (constant 202 mm × 202 mm illumination).

To demonstrate adsorption by the zeolite-coated muscovite, wafers which had undergone hydrothermal treatment (TEOS-Hyd and Hyd), as well as pieces of untreated muscovite (Musc) were washed for 1 h in 1% acetic acid (wt./vol.), then placed in 5 mL of 100 mg Ca L^{-1} calcium chloride solution. After a further period of 1 h the wafers were removed, washed with deionized water to remove residual $CaCl_2$ solution, and then dried at 45ºC. The wafers were then examined by light and scanning electron microscopy (Camscan Series 2 SEM with an EDX analyzer), and the chemical composition of surfaces was analyzed by energy dispersive analysis (SEM/EDX).

RESULTS

Physical description and sample weight change

After washing, the hydrothermally-treated muscovite wafers (TEOS-Hyd and Hyd) showed distinct differences between upper and lower surfaces. The face sandwiched against the glass-supporting plate was opaque, with white coloration, whilst the surface that faced downwards during hydrothermal treatment maintained some of its luster and reflected some light. This suggests that there is a difference between the materials deposited on the different sides. The presence of clusters of inter-planar material is also observed by light microscopy, where changing the focal length makes it possible to discriminate between deposition on the surface and within the muscovite wafers.

TEOS-treated wafers (TEOS) showed little or no detectable weight gain; however, significant changes in sample weight ($p < 0.05$) were observed in TEOS-Hyd and Hyd following hydrothermal treatment (Table 1), thus demonstrating a substantial deposition of material due to the hydrothermal treatment. However, statistical analysis, using a T test, of the changes in sample weight due to the hydrothermal treatments, *i.e.* between TEOS-Hyd and Hyd, show that there is no significant difference ($p > 0.05$) between the hydrothermal treatments, in terms of weight of material deposited, indicating that treatment with TEOS prior to hydrothermal treatment, as used in the TEOS-Hyd wafers, has no significant effect on quantity of deposition.

Alterations in composition

Analysis of the XRD patterns created during this study is difficult due to the complex nature of the potential mixtures, and the extreme degree of preferred orientation exhibited by all the wafers of muscovite. As the muscovite is a natural material with concomitant variation in chemical and physical composition, it is

Table 1. Mean change in sample weight per gram of muscovite for each of the treatments described.

Sample treatment	Mean (mg g^{-1})	σ
TEOS	1.0	1.1
TEOS-Hyd	39.8	7.1
Hyd	27.8	9.6

https://doi.org/10.1346/CCMN.2006.0540603 Published online by Cambridge University Press

difficult to get a crystal model which adequately describes the material. Total phase analysis by XRD is thus not possible, and therefore all analysis presented is qualitative. However, these results do give useful information on the changes and differences between the samples.

A search of structures using the Inorganic Crystal Structure Database (ICSD, Fletcher *et al.*, 1996) revealed three general structure types for muscovite designated by space group, and cited by reference to the simplest example. These are two monoclinic structures, $C2/c$ ($2M_1$) (Gatineau, 1960) and $C2/m$ ($1M$) (Sidorenko *et al.*, 1975) and one trigonal structure $P3_112$ ($3T$) (Güven and Burnham, 1966). The most abundant of these is the monoclinic $2M_1$ structure. Analysis of the ground randomized sample confirmed that the muscovite samples used in this study exhibit the $2M_1$ structure (Gatineau, 1960). This structure sets the direction of cleavage perpendicular to the c axis of the crystal. The cleaved wafers can therefore be thought of as a number of further cleavable slices, stacked in the c direction. Each slice is made up of one octahedrally bonded layer, surrounded by tetrahedrally bonded layers. The distribution of Al and Si within this sandwich determine the extent of charge compensation and K distribution in the interlayer zone. Cleavage is believed to occur in the K plane. Thus the formation of plates would be expected to cause preferred orientation with the 00*l* peaks exaggerated.

Analysis of the pattern for untreated muscovite wafer (Musc – Figure 1) shows that preferred orientation exaggerates three reflections which dominate the pattern. Three more peaks, which although smaller than the dominant peaks, are still substantially larger than any other reflections, are present in the pattern. Their positions show, as predicted, that they are related to the same reflection. The exaggerated reflections in the powder pattern are assigned to the 002, 004, 006, 008, 00,10 and 00,12 Miller planes.

The nature of the exaggerated peaks means that they display information on the disruption of order observed between cleavage planes in the sample. As faults appear and cleavage planes separate, broadening of these peaks would be expected as a result of stresses within the crystal and disruption of the ideal structure. The extent of this disruption will be related to the treatment undergone. The pre-treatment with TEOS should result in the deposition of a tiny layer of organosilicate, bonded to the silanol surface groups, wherever TEOS has penetrated between lamellae. This would be expected to produce only minor disruption. Hydrothermal treatment, on the other hand, should result in localized dissolution of lamellae surfaces, and deposition of zeolite crystals or X-ray amorphous gels with resulting disruption of the interlamellar stacking. This would be expected to result in more extensive disruption.

Comparison of the peak shapes of these strong reflections for the four types of material show important differences in the peak width and shape (Figure 2). For untreated muscovite, the peaks are sharp with a small peak width, but substantial tails appear after treatment, making the peak width at the base large. It is important to note that peaks are only broadened at the base. This suggests that layer disruption is not consistent throughout the sample, and that treatment results in a situation best modeled as a two-phase mixture, where resulting peaks are superimposed on each other. The two phases represent extremes: one highly crystalline, with a large

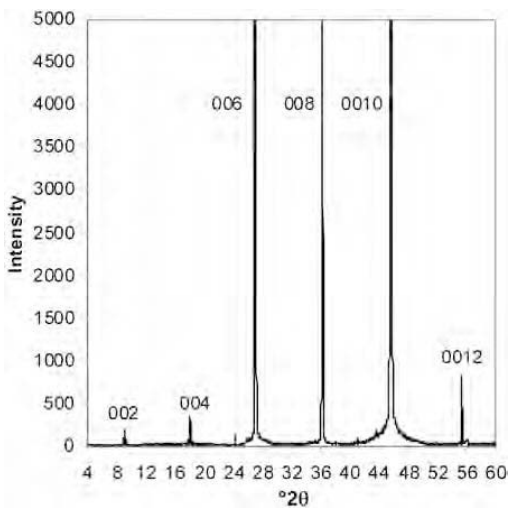

Figure 1. Muscovite XRD pattern showing peaks exaggerated by preferred orientation (peak heights for the largest peaks are 006 = 22800, 008 = 9500 and 00,10 = 43585).

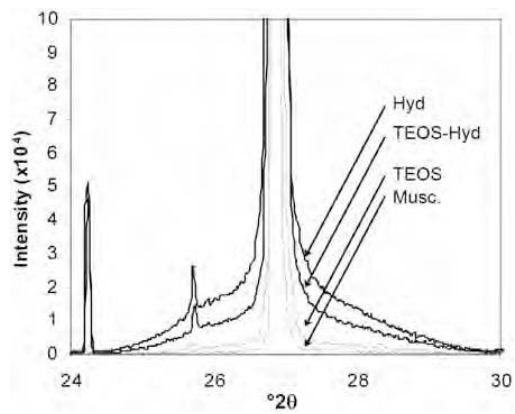

Figure 2. Peak broadening of the 004 and 006 reflections in untreated muscovite (Musc), TEOS-treated (TEOS), hydrothermally treated (Hyd), and TEOS and hydrothermally treated (TEOS-Hyd) muscovite samples

https://doi.org/10.1346/CCMN.2006.0540603 Published online by Cambridge University Press

Table 2. Relative peak heights for the dominant reflections in the XRD patterns of all samples normalized to the 00,10 peaks.

Sample	Relative height of peaks 00*n*					
	2	4	6	8	10	12
Musc	4	8	523	147	1000	19
TEOS	6	7	666	355	1000	72
TEOS-Hyd	11	330	919	793	1000	285
Hyd	1072	721	1066	696	1000	215

particle size, the other poorly crystalline with a small particle size. The first phase is consistent with the ideal stacking of planes leading to the narrowness of the upper sections of the peaks, and the second phase exhibits a large degree of amorphization and disruption of planes which results in the observed broadened peak tails. In addition, the treatments also have an affect on the intensity of the peaks observed; the relative intensities of the six peaks (Table 2) show major differences between each treatment. Hydrothermal treatments (TEOS-Hyd and Hyd) cause an increase in the relative heights of the peaks.

The peaks due to the 00*l* reflections were then modeled empirically and subtracted from the powder pattern to allow closer comparison of the residual pattern. When this was carried out, seven strong reflections (>1000 counts) remained in the pattern of the Hyd sample (Figure 3); the remaining samples (TEOS-Hyd, TEOS and Musc) showed some but not all of these reflections. Five of the strong reflections (Figure 3 – peaks 1–3, 5, 6) appear related to each other by an integral ratio of *d* spacings, the remaining two (Figure 3 – peaks 4, 7) appear not to be linked to the other reflections, or to each other. The different

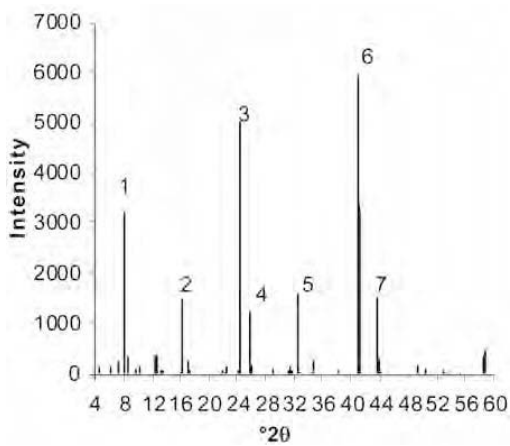

Figure 3. Residual peaks in the XRD pattern of a Hyd wafer, following the removal of dominant reflections caused by muscovite preferred orientation.

intensities of the peaks 1–3, 5 and 6 across all treatments (Table 3), and the absence of peaks 1 and 2 in calculated patterns of muscovite, suggest that these peaks are not actually related despite the apparent connections observed between the *d* spacings. Peaks present in the pattern of Musc and TEOS must be related to the muscovite. This is because no substantial alterations have occurred, except for very minor changes in the chemical composition of the immediate surface, and slightly increased disorder due to increased cleavage. Therefore, peaks 3–7 have been attributed to muscovite whilst the lower-angle peaks (peaks 1 and 2) are attributed to material introduced by hydrothermal synthesis. The peaks associated with muscovite were then modeled empirically and subtracted from the pattern, following which no further peaks were observed in the Musc or TEOS samples.

The residual pattern from the Hyd sample had evidence of several crystalline zeolite phases in the XRD pattern (Table 4). These have been identified by comparison with patterns in the ICDD powder diffraction file as probably belonging to Zeolite A ($Na_2Al_2Si_{1.85}O_{7.7}.5.1H_2O$ - PDF card no 38-241), Zeolite X ($Na_2Al_2Si_{2.5}O_9.6.2H_2O$ – PDF card no 38-237), Zeolite K-F ($Na_5Al_5Si_5O_{20}.9H_2O$ – PDF card no 39-217), and an unnamed zeolite ($Na_2Al_2Si_{5.7}O_{35.4}.8H_2O$ – PDF card no 35-375). Among those peaks attributable to a specific zeolite is the reflection at 16.12°2θ discussed previously (Table 3, Figure 3 – peak 2).

Due to the complex nature of this pattern and the small peak heights when compared to the muscovite substrate, with associated problems due to peak overlap, it has not been possible to collect enough evidence to identify the remaining peaks in the pattern conclusively, as several zeolite phases have major peaks corresponding with those remaining. However, the evidence points to the presence of at least four different zeolite phases associated with the matrix. Comparison of this finding with the XRD pattern of the powder remaining after

Table 3. Peaks heights of residual peaks in the XRD pattern of all samples following removal of the six most dominant reflections. Al peak heights are normalized to Peak 6, peaks marked N/P are not detectable on the XRD pattern.

Peak (2θ/*d*@peak max)	Treatments			
	Musc	TEOS	TEOS-Hyd	Hyd
1 (8.08/10.929)	N/P	N/P	N/P	544
2 (16.12/5.492)	N/P	N/P	N/P	250
3 (24.24/3.673)	1238	37	1060	852
4 (25.70/3.462)	972	117	339	207
5 (32.48/2.755)	N/P	53	N/P	266
6 (40.90/2.206)	1000	1000	1000	1000
(peak height)	(108)	(2645)	(4374)	(5932)
7 (43.48/2.080)	694	190	553	260

https://doi.org/10.1346/CCMN.2006.0540603 Published online by Cambridge University Press

Table 4. Residual peaks in the XRD pattern of Hyd samples following removal of peaks attributed to the muscovite base layer. Identified peaks have been assigned as Zeolite A (pdf card no 38-0241), Zeolite X (pdf card no 38-0237), Zeolite K-F (pdf card no. 39-0217), and unnamed zeolite $Na_5Al_5Si_5O_{20}.9H_2O$ (pdf card no 35-0375). Unassigned peaks are not conclusively attributable.

Hyd sample pattern *d* spacing (Å)	Zeolite A	Zeolite X	Zeolite K-F	Unnamed zeolite
19.6193				19.5975
14.5764		14.4716		
12.3011	12.2994			
10.9328				
10.4426				
10.3–8.8 obscured by 002 peak		8.8465		9.8456
8.6988	8.7142			
		7.5429		
7.0978	7.1109		7.1109	
6.6613			6.6813	
		5.7284	5.5642	
5.5003	5.5126			
5.2911				5.2510
5.1689				
5.08–4.76 Obscured by 004 peak	5.0317	4.8073	5.0254 4.8701	4.9111
	4.3619	4.4182	4.4958	4.3023
	4.2311		4.2138	
4.0994	4.1080		4.0155	4.0274
3.9937		3.9457		
3.4449	3.4159			
	3.7132	3.8065	3.7301	3.5895
		3.7645	3.5554	3.4159
		3.6086		
		3.5006		
3.39–3.25 Obscured by 006 peak	3.2924	3.3380 3.2532	3.3408	
			3.1799	3.1849
			3.1701	
			3.1385	
3.0909		3.0497	3.0227	
			3.0030	

hydrothermal treatment, which contains only zeolites A and X, suggests a site-specific growth, especially relating to zeolites F and the unnamed phase.

Similar deconstruction of the patterns from TEOS-Hyd wafers showed little evidence of crystalline zeolite phases, only a small number of peaks observed at lower *d* spacings; as with the residual peaks in the Hyd patterns, it is not possible to identify these peaks conclusively. However, it can be demonstrated that the residual powder from this hydrothermal treatment is identical to the Hyd residual. This further reinforces a site-specific growth theory, by demonstrating that masking of surface sites results in changes in crystal growth.

Surface formations

Analysis of the results from the SEM and SEM/EDX provides information on the surface formations, and allows the exploration of changes which occur on the upper and lower surfaces of the material during hydrothermal treatment. As mentioned in the physical description above, it is possible to distinguish with the naked eye the difference between the upper and lower surfaces of the hydrothermally treated fragments (TEOS-Hyd and Hyd). The differences between these surfaces are therefore discussed separately. This allows distinction between the two possible mechanisms for zeolite formation at the surface of the wafer. These mechanisms are the crystallization and bonding of material from the synthesis gel to the surface, or the zeolitization of the aluminosilicate muscovite directly to zeolite in the presence of NaOH. Both of these routes have been reported in the literature as mechanisms of zeolite film growth (Okada *et al.*, 2000, 2004).

Scanning electron microscopy images show that distinct differences exist in the extent of top surface reaction with the range of treatments (Figure 4). The surface of pure muscovite (Musc) is relatively featureless with only a few minor cracks and surface defects, and the TEOS sample shows little difference from this. The TEOS-Hyd and Hyd samples both show a distribution of small crystals across the surface; however, the comparison of crystal density between the TEOS-Hyd and Hyd wafers shows a marked difference. In the TEOS-Hyd sample, surface density is variable from a relatively low abundance (Figure 4d) to dense patches of crystals (Figure 4e). These patches are clearly identifiable by variation in shading of the low-magnification image (Figure 4c) with the light areas being areas of greater abundance. In comparison, the Hyd wafer has a complete film of interlocking crystals across the whole surface; this is visible in the high-magnification image (Figure 4f).

The interlocking nature of these crystals is quite distinct from even the high-abundance areas observed in TEOS-Hyd. The crystals observed in both samples appear angular, probably cubic or octagonal in nature. This density difference is supported by the results of the SEM/EDX analysis (Table 5). A T test carried out on these data shows a significant increase in the SiO_2/Al_2O_3 ratio ($p < 0.05$) between the surface of Musc wafers and the upper surface of both hydrothermally treated (TEOS-Hyd and Hyd) wafers, whilst increasing amounts of Na and a reduction in K also indicate reaction between the surface and the synthesis gel. The change is more pronounced in the Hyd sample than in TEOS-Hyd, providing further indication that film growth is more complete in the former sample. There is no significant difference ($p > 0.05$) in the SiO_2/Al_2O_3 ratio or concentration of K between the untreated Musc and TEOS-treated wafers. It has not been possible to examine the nature of the adhesion between interlocked crystals and

https://doi.org/10.1346/CCMN.2006.0540603 Published online by Cambridge University Press

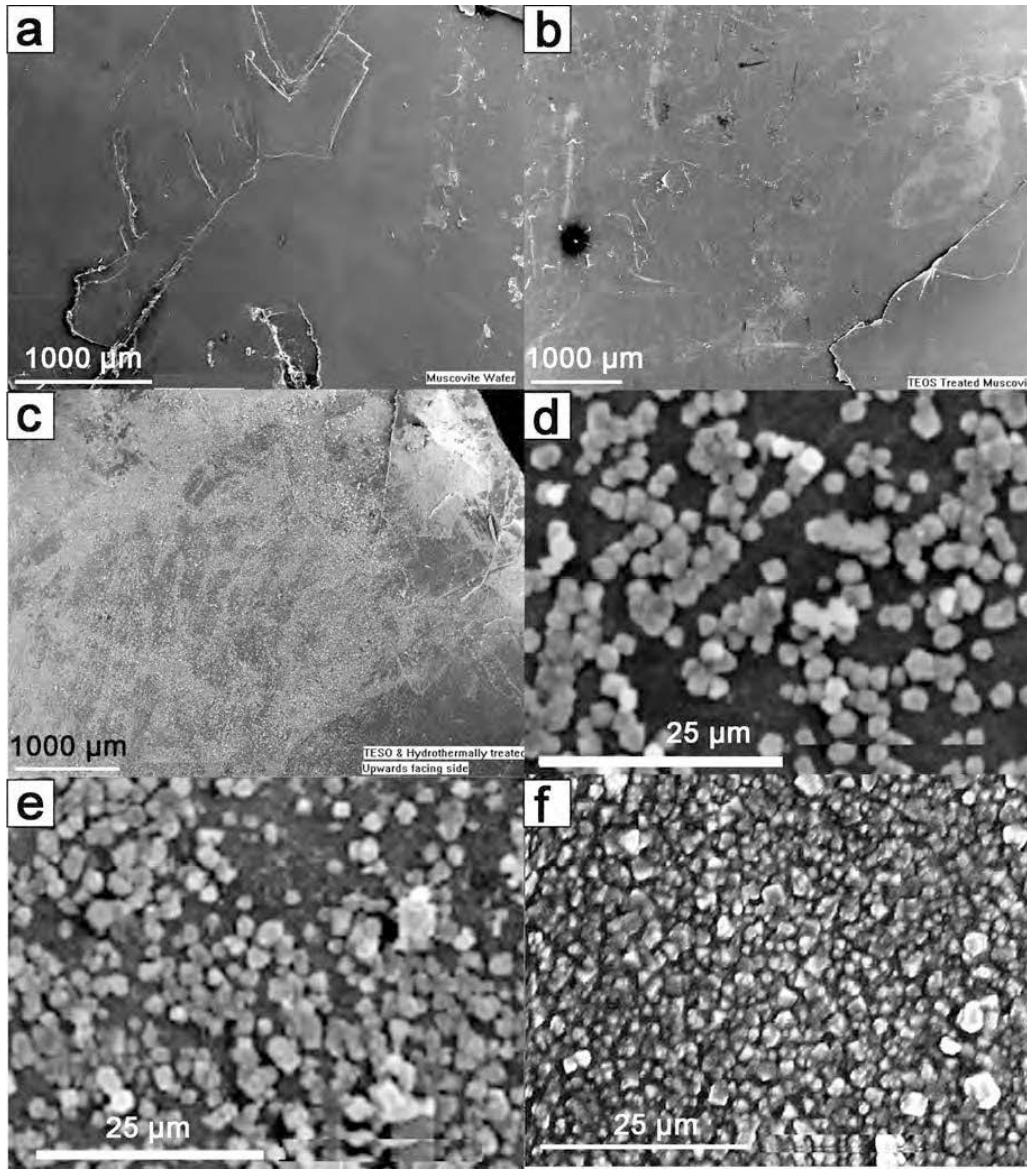

Figure 4. SEM images of the surface of an untreated muscovite wafer (a); TEOS-treated muscovite (b), and of the surface uppermost during the hydrothermal treatment of TEOS-Hyd (c–e) and Hyd (f), demonstrating the presence and variation in the density of the zeolite film growth.

the clay surface directly by TEM of the cross-section view due to the use of a perfectly cleavable substrate, which means that in cross section it is impossible to distinguish between cleavage due to sample preparation, and any non-adhesion of the surface layers.

The differences between the upper and lower surfaces of the hydrothermally treated materials (TEOS-Hyd and Hyd) are also visible from the SEM images of the downward-facing surface (Figure 5). Especially of note is a distinct difference in the TEOS-Hyd samples, the downward-facing surface of which (Figure 5a) is almost entirely clear of deposited material, in comparison to that of the Hyd wafer (Figure 5b–d) where some interlocked deposition occurs in small patches, but it

https://doi.org/10.1346/CCMN.2006.0540603 Published online by Cambridge University Press

Table 5. SEM/EDX analysis showing elemental composition of muscovite, TEOS-treated muscovite (TEOS), and the surface uppermost during the hydrothermal treatment of TEOS pretreated (TEOS-Hyd) and plain (Hyd) muscovite.

Sample	Analyte	Mean %	σ
Musc	Na	0	0
	Al_2O_3	27.52	0.28
	SiO_2	57.54	0.24
	K_2O	12.62	0.29
	Fe_2O_3	2.31	0.14
TEOS	Na	0	0
	Al_2O_3	27.68	0.15
	SiO_2	57.67	0.20
	K_2O	12.51	0.07
	Fe_2O_3	2.13	0.21
TEOS-Hyd	Na	0.45	0.06
	Al_2O_3	27.39	0.21
	SiO_2	59.56	0.53
	K_2O	10.76	0.38
	Fe_2O_3	1.88	0.20
Hyd	Na	1.38	0.21
	Al_2O_3	28.11	0.34
	SiO_2	64.69	2.16
	K_2O	4.43	1.81
	Fe_2O_3	1.19	0.81

does not form a complete film due to regions where no reaction has occurred. The SEM/EDX confirms the difference in chemical composition by analyzing Na concentration as a proxy for gel reaction (Table 6). This shows a significant difference ($p < 0.05$) not only between the upper and lower surfaces, but between light and dark regions on the Hyd wafer.

Adsorption of cations

Analysis of the exchanged samples by SEM/EDX (Table 7) shows clear evidence of Ca uptake by both hydrothermally treated wafers (TEOS-Hyd and Hyd). Furthermore, a considerable difference exists between the uptake of Ca by the upper and lower surfaces of the wafer.

Table 7. SEM/EDX analysis of Ca-exchanged wafers showing the uptake of Ca and chloride from solution. Atom % given as *before* and after exchange where appropriate.

Sample	Atom	Mean at.%	σ
Musc	Na	*0* 0	0
	Ca	*0.20*	0.35
	Cl	0	0
TEOS-Hyd (upside)	Na	*0.77* 0	0
	Ca	1.52	0.90
	Cl	5.48	2.32
TEOS-Hyd (downside)	Na	*0.5* 0	0.11
	Ca	0.13	0.22
	Cl	0.86	0.42
Hyd (upside)	Na	*2.82* 0	0
	Ca	1.41	0.41
	Cl	0.27	0.25
Hyd (downside)	Na	*1.0* 0.39	0.07
	Ca	0	0
	Cl	0.15	0.25

Ion exchange between zeolite and solution would lead to the replacement of extra-framework Na ions with Ca. This exchange should have no effect on the appearance of the solution counter ion (Cl^- in this instance) on the surface of the material. The detection of increased Cl at the surface of the material would indicate that some Ca adsorbed requires the continued presence of its counter ion to allow charge balance. Analysis by SEM/EDX demonstrates a significant difference ($p < 0.05$) between the chloride content of the TEOS-Hyd and Hyd samples, suggesting that the mechanism for Ca uptake is different for each preparation, with ion exchange being the more likely mechanism in the Hyd samples. This supports the evidence of both XRD and SEM which indicated a less well formed surface on the TEOS-Hyd samples.

Table 6. Comparison of elemental composition of upper and lower surfaces of hydrothermally treated muscovite wafers with and without TEOS pre-treatment (TEOS-Hyd and Hyd, respectively) by SEM/EDX.

Sample	Analyte	Mean % up (down)	σ up (down)
TEOS-Hyd	Na	0.45 (0.02)	0.06 (0.04)
	K_2O	10.72 (12.00)	0.21 (0.13)
	SiO_2/Al_2O_3	3.84 (3.67)	0.06 (0.06)
Hyd[†]	Na	1.38 (0.07 *1.04*)	0.21 (0.06 *0.07*)
	K	4.43 (12.15 *6.50*)	1.81 (0.12 *0.57*)
	SiO_2/Al_2O_3	4.08 (3.72 *3.84*)	0.18 (0.07 *0.03*)

[†]The two distinct areas which exist on the down-facing surface of Hyd sample, characterized by the coloration of SEM images, are treated separately as dark and *light*.

https://doi.org/10.1346/CCMN.2006.0540603 Published online by Cambridge University Press

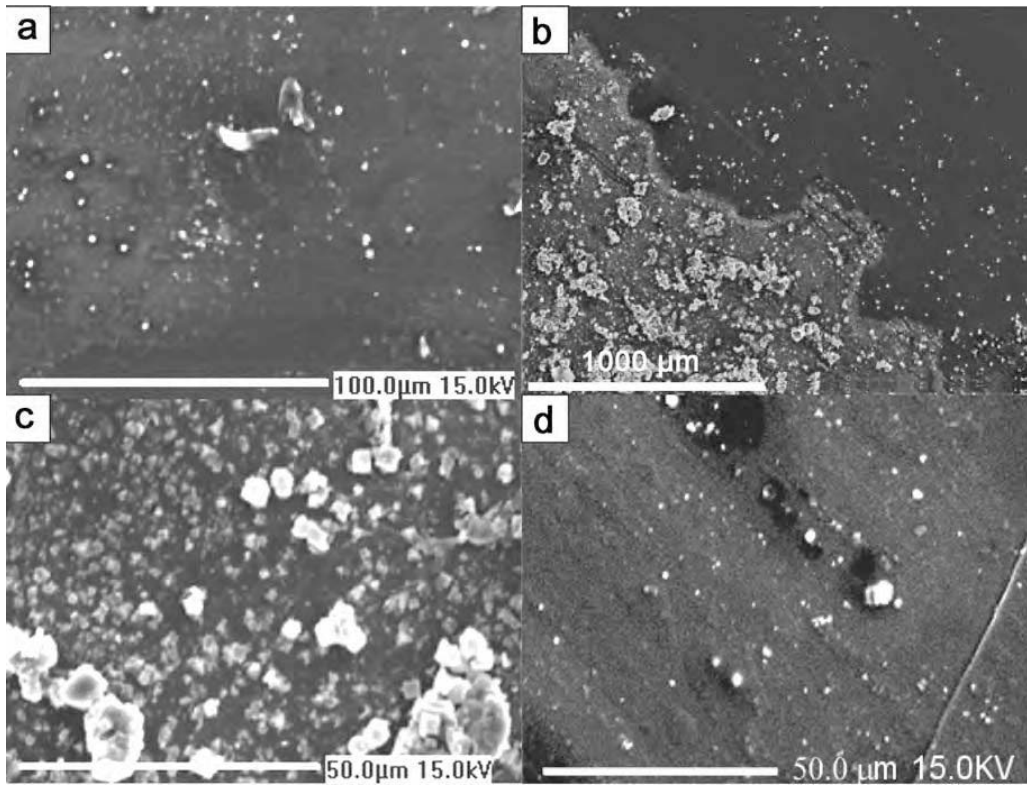

Figure 5. SEM images of the surface of TEOS-Hyd (a) and Hyd (b–d) wafers which faced downwards during hydrothermal treatment, showing the extent and variability of zeolite film growth. Differentiation between light (c) and dark (d) areas of the Hyd wafer (b) is observed.

DISCUSSION

The results of this study provide several insights into the mechanisms and extent of zeolitization which occur when an aluminosilicate substrate is hydrothermally treated. These offer an important insight when considering optimization of the surface for metal adsorption. The discussion of this study can therefore be divided into two principal areas.

Degree of zeolitization

The degree of zeolitization must be examined in the context of the whole wafer, as it is this that will be used as a metal-adsorption product. The weight gain of the samples showed no statistical difference between either hydrothermal treatment, although weight gain was greater when the wafer was pretreated (TEOS-Hyd) than when hydrothermal treatment alone was used (Hyd). However, when the XRD evidence is included, there are real differences between the samples with regard to the presence of crystalline zeolite. In addition, the SEM clearly shows that the densities of zeolite on the surfaces of the material are different, with a continuous interlocked layer of crystalline material observed in the Hyd wafer, compared with a lower and variable density of individual crystals present on TEOS/Hyd.

There are two obvious explanations for this result; either the weight gain is enhanced in TEOS-Hyd by the presence of an X-ray amorphous or poorly crystalline material within the mica interlayers, where it is not observed by the SEM; or the increased zeolitization observed in Hyd wafers can be attributed to the conversion of muscovite layers into zeolite, enhancing the zeolite content with little associated weight gain. As it is not possible to calculate the amorphous content, the only evidence which would indicate one mechanism or the other is the disruption of the cleavage planes, observed from the peak tails. The sizes of these tails are greater for the Hyd sample, indicating that there is less disruption to the muscovite structure in TEOS-Hyd. Without further evidence, this suggests that some muscovite conversion is taking place on the Hyd sample, leading to disruption of the structure, but a substantially larger zeolite content and better formed films. Furthermore, the level of disruption also indicates that more zeolitization is occurring between the planes in Hyd than in TEOS-Hyd.

https://doi.org/10.1346/CCMN.2006.0540603 Published online by Cambridge University Press

Mechanisms of zeolitization

The mechanism of zeolitization is a surface phenomenon, and changes to the nature of this surface appear to have substantial effects on the zeolitization. This is observed in the apparent surface specific growth seen in the diffraction patterns.

Differences observed due to sample orientation suggest the mechanism of zeolitization. There is evidence in the literature (Okada *et al.*, 2000) for the direct transformation of an aluminosilicate substrate to a zeolite film in the presence of concentrated NaOH. The other possible mechanism in this system is the crystallization of deposited precursor and the bonding of this to the surface. The fact that the degrees of zeolite deposition on the upper and lower surfaces are different proves that the zeolitization of the surface cannot occur by interaction of the muscovite with the NaOH liquor alone, as the conditions on the upper and lower surfaces of the wafer with respect to NaOH are identical. Although in the Hyd sample some deposition is observed on the bottom surface, this is not nearly as continuous as on the top and there are large sections where no deposition occurred. However, in some areas it has bonded to the surface to form interlocked films similar to those on the top surface, indicating that once nucleation has occurred, film growth is not surface specific. On the top surface, where synthesis gel becomes trapped between the glass support and the muscovite wafer, nucleation occurs more evenly resulting in a better surface coverage.

However, having proposed that the zeolite film growth proceeds from the ageing of a deposited precursor, it is vital to note the evidence presented when examining the degree of zeolitization. This suggests a requirement for some degree of surface-phase transformation. The observation is not wholly consistent with a growth mechanism relying solely on the nucleation of the crystal within a precursor gel. It is therefore necessary to examine further the evidence for the chemical interaction of the muscovite surface with the growing zeolite film. Comparison of TEOS-Hyd and Hyd wafers provides an insight into this. Treatment of the surface with TEOS should ensure that the immediate surface of the material was predominantly silica bound in a very fine layer. This has a substantial effect on the nucleation. The SEM images of TEOS-Hyd show no signs of continuous film growth, although there are clusters of crystals adhered to the top surface in patches of uneven density. The treatment with TEOS has therefore had some effect on retardation of complete film growth; this is also supported by the complete absence of crystals on the lower surface indicating no reaction where the precursor was not held firmly in contact with the substrate. Furthermore, the XRD patterns of the TEOS-Hyd wafers showed no discernable peaks due to the presence of zeolites indentified on the Hyd wafer. The site-specific nucleation theory is also supported by the presence of at least four zeolitic phases in the XRD patterns of the Hyd film, whereas only two occur in the residual powder. This suggests that the zeolitic composition of the wafer is not just a mirror of the synthesis powder composition. Should this be the case, it highlights a problems with using natural materials with a variable composition as hosts for films where less phase variation is tolerated.

It is therefore proposed that the interaction of the precursor with the muscovite surface and subsequent formation of interlocking zeolite layers is due to the interaction of the precursor gel with sites on the muscovite surface. Blocking of these sites will lead to the prevention of film growth over large areas. Once film growth has been initiated, the muscovite surface degradation and subsequent integration of the film into the substrate can occur, with zeolite growth not necessarily controlled by the zeolitic composition of the crystallizing synthesis gel. It is also proposed that the development of strongly adhered films on many substrates must therefore depend on appropriate sites of bonding being available, and that it is not necessarily sufficient to provide any nucleation surface.

Changes in physical properties

The cation adsorption experiment carried out in this study shows that although enhanced adsorptive properties have been introduced to regions of the surface, it has not been possible to deposit enough zeolite to have a substantial impact. The properties of this lamellar material provide some further difficulties. As the amount of material in the cleavage planes increases, a reaction which is necessary for any increase in the amount of zeolite present and thus the adsorption capacity, total separation of cleavage layers can occur. This may lead to a delaminated product held together lightly by the material between the plates. A more ideal material must have a greater space between the cleavage planes allowing the formation of zeolite in pockets without causing total separation and delamination of the material, with subsequent loss of the mechanical stability which was a fundamental requirement for using a supported film. The use of muscovite, therefore, only offers a partial solution to the problems faced, but more importantly, its use has demonstrated what is potentially achievable.

CONCLUSIONS

This study has demonstrated that the attachment of the zeolite to relatively robust and flexible support media is possible, and therefore that a muscovite mica can be treated to give it increased cationic adsorption. It has succeeded in providing a synthetic zeolitic material that does not have the same issues of micro-filtration and physical handling as a synthetic powder. However, the adhesion and crystallization processes are both dependent on suitable nucleation sites being present on the

https://doi.org/10.1346/CCMN.2006.0540603 Published online by Cambridge University Press

clay surface. Masking these sites leads to patchy deposition of more poorly crystalline material. However, clay minerals as growth media appear to offer these sites and thus provide a good level of adhesion between the zeolite and clay support matrix as demonstrated by the film's resistance to a relatively aggressive washing and characterization process.

The detection of Na and Ca in the film growth areas of the mineral surface suggests that cation adsorption has been increased substantially. As only a tiny amount of zeolite was added to the muscovite, the increased adsorption is seriously limited. This research indicates that zeolitization of lamellar clay minerals could provide useful materials if a more suitable substrate was identified.

ACKNOWLEDGMENTS

The support of Dr John Evans in the Department of Chemistry for use of X-ray diffraction facilities is acknowledged. The authors also thank Dr Janet Skakle at the University of Aberdeen for her support and advice. The authors wish to acknowledge the use of the EPSRC Chemical Database Service, Daresbury, UK (Fletcher *et al.*, 1996). This work was funded by the County Durham Environment Trust (CDENT).

REFERENCES

Caro, J., Noack, M., Kölsch, P. and Schäfer, R. (2000) Zeolite membranes – state of their development and perspective. *Microporous and Mesoporous Materials*, **38**, 3–24.

Cui, Y., Kita, H. and Okamoto, K.-I. (2003) Preparation and gas separation properties of zeolite T membrane. *Chemical Communications*, 2154–2155.

Cui, Y., Kita, H. and Okamoto, K.-I. (2004a) Zeolite T membrane: preparation, characterisation, pervaporation of water/organic liquid mixtures and acid stability. *Journal of Membrane Science*, **236**, 17–27.

Cui, Y., Kita, H. and Okamoto, K.-I. (2004b) Preparation and gas separation performance of zeolite T membrane. *Journal of Materials Chemistry*, **14**, 924–932.

Coutinho, D. and Balkus Jr., K.J. (2002) Preparation and characterization of zeolite X membranes via pulsed-laser deposition *Microporous and Mesoporous Materials*, **52**, 79–91.

Deng, Z. and Balkus Jr., K.J. (2002) Pulsed laser deposition of zeolite NaX thin films on silica fibers. *Microporous and Mesoporous Materials*, **56**, 47–53.

Fletcher, D.A., McMeeking, R.F. and Parkin, D. (1996) The United Kingdom Chemical Database Service. *Journal of Chemical Information and Computer Sciences*, **36**, 746.

Gatineau, L. (1960) Localisation des remplacements isomorphiques dans la Muscovite. *Acta Crystallographica*, **13**, 919–932.

Güven, N. and Burnham, C.W. (1966) The crystal structure of 3T muscovite. *Carnegie Institution of Washington Yearbook*, **65**, 290–293.

Hedlund, J., Mintova, S. and Sterte, J. (1999) Controlling the preferred orientation in silicalite-1 films synthesized by seeding. *Microporous and Mesoporous Materials*, **28**, 185–194.

Huang, A., Ling, Y.S. and Yang, W. (2004) Synthesis and properties of A-type zeolite membranes by secondary growth method with vacuum seeding. *Journal of Membrane Science*, **245**, 41–51.

Johnson, C.D. and Worrall, F. (2004) Chemical pore closure of zeolite A using tetraethyl orthosilicate: A potential method for enhancing the use of zeolites as part of a long term waste immobilization strategy. *Microporous and Mesoporous Materials*, **73**, 191–196.

Johnson, C.D., Macphee, D.E. and Feldmann, J. (2002) New low temperature synthetic route to an ammonium zinc arsenate zeolite analogue with an ABW type framework. *Inorganic Chemistry*, **41**, 3588–3589.

Johnson, C.D., Johnson, D.C. and Worrall, F. (2004) Influence of processing of natural zeolite upon metals removal capacity. *Proceedings of REWAS 2004, Global Symposium on Recycling, Waste Treatment and Clean Technology*, **2**, 1819–1828.

Kyaw, K., Shibata, T., Watanabe, F., Matsuda, H. and Hasatani, M. (1997) Applicability of zeolite for CO_2 storage in a CaO-CO_2 high temperature energy storage system. *Energy Conversion and Management*, **38**(10–13), 1025–1033.

Langella, A., Pansini, M., Cappelletti, P., de' Gennaro, B., de' Gennaro M. and Colella, C. (2000) NH_4^+, Cu^{2+}, Zn^{2+}, Cd^{2+} and Pb^{2+} exchange for Na^+ in a sedimentary clinoptilolite, North Sardinia, Italy. *Microporous and Mesoporous Materials*, **37**, 337–343.

Lassinantti, M., Hedlund, J. and Sterte, J. (2000) Faujasite-type films synthesized by seeding. *Microporous Mesoporous Materials*, **38**, 25–34.

Masuda, T., Otani, S.-h., Tsuji, T., Kitamura, M. and Mukai, S.R. (2003) Preparation of hydrophilic and acid-proof silicalite-1 zeolite membrane and its application to selective separation of water from water solutions of concentrated acetic acid by pervaporation. *Separation and Purification Technology*, **32**, 181–189.

Mondale, K.D., Carland, R.M. and Aplan, F.F. (1995) The comparative ion exchange capacities of natural sedimentary and synthetic zeolites. *Minerals Engineering*, **8(4/5)**, 535–548.

Murat, M., Amorkane, A., Bastide, J.P. and Montanaro, L. (1992) Synthesis of zeolites from thermally activated kaolinite – some observations on nucleation and growth. *Clay Minerals*, **27**, 119–130.

Okada, K., Kuboyama, K.-I, Takei, T., Kameshima, Y., Yasumori, A. and Yoshimura, M. (2000) In situ zeolite Na-X coating on glass fibers by soft solution process. *Microporous and Mesoporous Materials*, **37**, 99–105.

Okada, K., Kameshima, Y., Madhusoodana, C.D. and Das, R.N. (2004) Preparation of zeolite-coated cordierite honeycombs prepared by an in situ crystallization method. *Science and Technology of Advanced Materials*, **5**, 479–484.

Sayari, A., Hamoudi, S. and Yang, Y. (2005) Applications of pore-expanded mesoporous silica. 1. Removal of heavy metal cations and organic pollutants from wastewater. *Chemistry of Materials*, **17**, 212–216.

Sidorenko, O.V., Zvyagin, B.B. and Soboleva, S.V. (1975) Crystal structure refinement for 1M dioctahedral mica. *Krystallografiya*, **20**, 543–549.

Xu, Y., Ohki, A. and Maeda, S. (1998) Adsorption of arsenic(V) by use of aluminium-loaded Shirasu-Zeolites. *Chemistry Letters*, 1015.

(*Received 4 August 2005; revised 16 May 2006; Ms. 1089; A.E. Peter J. Heaney*)